Optical and Acoustic Studies of pH-Dependent Swelling in Microgel Thin Films

Michael J. Serpe and L. Andrew Lyon*

School of Chemistry and Biochemistry, Georgia Institute of Technology, Atlanta, Georgia 30332-0400

Received July 15, 2004. Revised Manuscript Received August 30, 2004

We report investigations on the swelling behavior of poly(*N*-isopropylacrylamide-*co*-acrylic acid) (pNIPAm-*co*-AAc) microgel thin films as a function of pH using quartz crystal impedance (QCI) analysis and surface plasmon resonance (SPR) spectroscopy. In this work, pNIPAm-*co*-AAc microgels are assembled into thin films using a spin-coating layer-by-layer (scLbL) assembly approach by alternatively exposing 2-mercaptoethylamine-functionalized Au QCI and SPR substrates to polyanionic pNIPAm-*co*-AAc microgels and polycationic poly(allylamine hydrochloride). The scLbL process is followed by QCI analysis, which displays a linear decrease in resonant frequency, i.e., increase in mass, as a function of the microgel layer number. The swelling behavior of an assembled film in response to acidic (pH $\approx$ 3.0) and neutral (pH $\approx$ 6.5) solution conditions is monitored using QCI. Exposure of a microgel thin film to acidic solution results in a dramatic decrease in resonant frequency and an increase in motional resistance. When this same film is exposed to a neutral pH solution, the resonant frequency and resistance of the quartz again decrease and increase, respectively, but with the changes being more dramatic than those of the film in acidic solution. This behavior is believed to be due to the film transitioning from a highly solvent swollen state under acidic conditions to a less swollen state near neutral pH. To confirm this interpretation, SPR measurements were performed, which suggest that the film is less optically dense under acidic conditions, i.e., more solvent swollen, than the same film at pH $\approx$ 6.5. This differential solvation behavior is highly reversible, with the solvation/desolvation rates being dependent on the number of microgel layers in the film.

Introduction

Responsive hydrogel thin films are cross-linked, solvent-swollen, polymeric materials that undergo solvation changes in response to the application of an external stimulus.[1−3] The responsivity of a hydrogel arises from competing solvation mechanisms, where under one condition the network polymer chains are fully solvent swollen but upon introduction of an external stimulus the favorable polymer−solvent interactions are disrupted and polymer−polymer interactions begin to dominate, causing the polymer network to aggregate and deswell. This behavior is known as a volume phase transition (VPT) and is analogous to the coil-to-globule transition seen in linear poly(*N*-isopropylacrylamide) (pNIPAm) near that polymer's lower critical solution temperature (LCST) of ∼31 °C.[4] The fundamental properties of thermoresponsive/pH-responsive hydrogel systems have been studied extensively and reviewed previously.[5,6] Thin pNIPAm hydrogel films have been studied with respect to the deswelling mechanism and kinetics[7,8] and hydrogel composition[9−11] using techniques such as surface plasmon resonance spectroscopy,[12,13] quartz crystal microbalance measurements,[14,15] light scattering/turbidimetry,[8,9] differential scanning calorimetry,[11] and microscopy.[10]

In this investigation we use hydrogel microparticles (microgels) composed of a random copolymer of *N*-isopropylacrylamide (NIPAm) and acrylic acid (AAc) cross-linked with *N*,*N*′-methylenebis(acrylamide) to construct microstructured, hydrogel thin films. Microgels composed of pNIPAm are very well studied materials that undergo a reversible temperature-induced collapse at ∼31 °C.[5,6,16,17] The addition of AAc into the microgel

* To whom correspondence should be addressed. E-mail: lyon@chemistry.gatech.edu.

(1) Miyata, T.; Asami, N.; Uragami, T. *Nature* **1999**, *399*, 766−769.
(2) Kokufata, E.; Zhang, Y. Q.; Tanaka, T. *Nature* **1991**, *351*, 302−304.
(3) Oya, T.; Enoki, T.; Grosberg, A. Y.; Masamune, S.; Sakiyama, T.; Takeoka, Y.; Tanaka, K.; Wang, G.; Yilmaz, Y.; Feld, M. S.; Dasari, R.; Tanaka, T. *Science* **1999**, *286*, 1543−1545.
(4) Wu, C.; Zhou, S. *Macromolecules* **1995**, *28*, 8381−8387.
(5) Saunders, B. R.; Vincent, B. *Adv. Colloid Interface Sci.* **1999**, *80*, 1−25.
(6) Pelton, R. *Adv. Colloid. Interface Sci.* **2000**, *85*, 1−33.
(7) Yan, Q.; Hoffman, A. S. *Polym. Commun.* **1995**, *36*, 887−889.
(8) Tanaka, T.; Sato, E.; Hirokawa, Y.; Hirotsu, S.; Peetermans, J. *Phys. Rev. Lett.* **1985**, *55*, 2455−2458.
(9) Nayak, S.; Debord, S. B.; Lyon, L. A. *Langmuir* **2003**, *19*, 7374−7379.
(10) Chen, J.; Park, H.; Park, K. *J. Biomed. Mater. Res.* **1999**, *44*, 53−62.
(11) Cai, W. S.; Gupta, R. B. *J. Appl. Polym. Sci.* **2002**, *83*, 169−178.
(12) Harmon, M. E.; Jakob, T. A. M.; Knoll, W.; Frank, C. W. *Macromolecules* **2002**, *35*, 5999−6004.
(13) Harmon, M. E.; Kuckling, D.; Pareek, P.; Frank, C. W. *Langmuir* **2003**, *19*, 10947−10956.
(14) Plunkett, M. A.; Wang, Z. H.; Rutland, M. W.; Johannsmann, D. *Langmuir* **2003**, *19*, 6837−6844.
(15) Calvo, E. J.; Danilowicz, C.; Etchenique, R. *J. Chem. Soc., Faraday Trans.* **1995**, *91*, 4083−4091.

10.1021/cm048844v CCC: $27.50
Published on Web 10/09/2004

network, via copolymerization, results in modulation of the VPT at pH values greater than the AAc pK_a (4.25). At these pH values, the VPT shifts to higher temperature due to deprotonation of the AAc groups, which introduces Coulombic repulsion and a high Donnan potential inside the network.[17,18]

Microstructured, hydrogel thin films used in this investigation were made by a spin-coating layer-by-layer (scLbL) assembly approach. Each layer was added sequentially by dripping a specific volume of each polymer solution onto a spinning substrate with H_2O rinses between each polymer layer addition.[19,20] Traditionally assembled LbL microgel thin films have previously been shown to exhibit pH-dependent thermoresponsivity, where at pH 3.0 the films were shown to be thermoresponsive while at pH 6.5 the films exhibited hindered thermoresponsivity.[21] This behavior was explained by taking into account the pH responsivity of the discrete microgels in the film, where at pH 3.0 (pH < pK_a of AAc) the microgel AAc groups are mostly protonated and the microgel is therefore able to deswell unhindered at ~31 °C, whereas at pH 6.5 (pH > pK_a) the microgels were mostly deprotonated and therefore less thermoresponsive over the same temperature range. To a first approximation, consideration of the isolated microgel behavior in response to pH is an attractive way to analyze the data. However, this does not take into account the complex ionic interactions between the linear polyelectrolyte and microgel, as their charge densities change with pH.

Molecular-scale ionic interactions have previously been investigated for traditionally assembled[22,23] polyelectrolyte multilayer thin films composed of weak polyacids/bases.[24−28] These investigations found that the polyelectrolyte layer conformation is highly dependent on the ionic strength and pH of the polyelectrolyte deposition solution. For example, polyelectrolyte layer deposition from a solution where the polyelectrolyte is not fully charged results in a layer with a thick, "loopy" conformation, whereas deposition from a solution that enforces polyelectrolyte ionization results in a thin, more rigid layer.[25] This can be understood by considering the number of ionic interactions necessary to neutralize the underlying polyelectrolyte layer and reverse the charge on the surface. Under low ionization conditions the layers deposit with fewer side chain−side chain interactions, leaving loopy polymer segments. This results in an overall thicker film. Under high ionization conditions, the layers interact very strongly with a high number of interactions, resulting in a rigid, thin layer.[25,28] Studies have also been performed to understand the effect of solution pH on LbL film swelling.[24,29−31] These investigations have shown that, when a polyelectrolyte film was exposed to a low-pH solution, the film became thicker due to disruption of the ionic interactions within the film. This results in film swelling and in some cases disassembly. If the film was subsequently exposed to a high-pH solution, the film rigidified due to enforced ionic interactions. The above results illustrate the fact that solution pH and ionic strength play major roles in the resultant morphology and behavior of polyelectrolyte thin films, and that the ionic interactions within polyelectrolyte thin films can be dynamically tunable and reversible. In this study we investigate the effect of solution pH on the swelling behavior of scLbL microgel thin films. This particular polyelectrolyte system is slightly different from traditional LbL-assembled thin films because (1) the layers are applied by spin coating rather than passive adsorption and (2) one of the polyelectrolytes is a microgel network particle as opposed to a linear polyelectrolyte. Nonetheless, quartz crystal impedance (QCI) and surface plasmon resonance (SPR) analyses suggest that much of the pH-dependent behavior observed previously for linear polyelectrolyte films is also operative in the present case.

Experimental Section

Materials. All reagents were purchased from Sigma-Aldrich unless otherwise specified. NIPAm was recrystallized from hexanes (J.T. Baker) and dried under vacuum prior to use. AAc was distilled under reduced pressure. *N*,*N*′-Methylenebis-(acrylamide) (BIS) and ammonium persulfate (APS) were used as received. Poly(allylamine hydrochloride) (PAH), MW 70000, was used as received. 2-Mercaptoethylamine (MEA) was used as received and stored at 4 °C. Polished quartz crystals (5.0 MHz AT-cut) were purchased from International Crystal Manufacturing (Oklahoma City, OK). Cuvettes used were obtained from VWR. Au (99.999% pure) was obtained from Alfa Aesar. Glass substrates were 24 × 24 mm Fisher Finest brand cover glass obtained from Fisher Scientific. Ethanol (95% and absolute) was used for various purposes in this investigation. All water used throughout this investigation was house distilled, then deionized to a resistance of at least 18 MΩ (Barnstead Thermolyne E-Pure system), and then filtered through a 0.2 μm filter for further purification.

Quartz Crystal Impedance Measurements and Thin Film Deposition. For this study ~5 MHz AT-cut quartz crystals were used with a standard keyhole electrode configuration. The electrode area of 0.0951 cm^2 gives a mass sensitivity of 1.68 ng/Hz, as calculated using the Sauerbrey equation (eq 1),

$$\Delta f_p = -2 f_{p_0}{}^2 \Delta m / A(\mu_q \rho_q)^{1/2} \quad (1)$$

where Δf_p is the measured frequency shift, f_{p_0} is the frequency of the quartz crystal prior to mass addition, Δm is the mass change, A is the electrode area, and μ_q and ρ_q are the shear modulus and density of quartz, respectively. Before polyelectrolyte deposition, the Au electrodes were rendered positively charged using well-known thiol self-assembly methods.[32] Specifically, the substrates were immersed in a 1.0 mM

(16) Gan, D. J.; Lyon, L. A. *J. Am. Chem. Soc.* **2001**, *123*, 7511−7517.
(17) Jones, C. D.; Lyon, L. A. *Macromolecules* **2000**, *33*, 8301−8306.
(18) Morris, G. E.; Vincent, B.; Snowden, M. J. *J. Colloid Interface Sci.* **1997**, *190*, 198−205.
(19) Lee, S. S.; Lee, K. B.; Hong, J. D. *Langmuir* **2003**, *19*, 7592−7596.
(20) Chiarelli, P. A.; Johal, M. S.; Holmes, D. J.; Casson, J. L.; Robinson, J. M.; Wang, H. L. *Langmuir* **2002**, *18*, 168−173.
(21) Serpe, M. J.; Jones, C. D.; Lyon, L. A. *Langmuir* **2003**, *19*, 8759−8764.
(22) Decher, G. *Science* **1997**, *277*, 1232−1237.
(23) Decher, G.; Hong, J. D. *Ber. Bunsen-Ges.* **1991**, *95*, 1430−1434.
(24) Tanchak, O. M.; Barrett, C. J. *Chem. Mater.* **2004**, ACS ASAP.
(25) Shiratori, S. S.; Rubner, M. F. *Macromolecules* **2000**, *33*, 4213−4219.
(26) Xie, A. F.; Granick, S. *J. Am. Chem. Soc.* **2001**, *123*, 3175−3176.
(27) Rmaile, H. H.; Schlenoff, J. B. *Langmuir* **2002**, *18*, 8263−8265.
(28) Yoo, D.; Shiratori, S. S.; Rubner, M. F. *Macromolecules* **1998**, *31*, 4309−4318.
(29) Kim, B.-S.; Vinogradova, O. I. *J. Phys. Chem. B* **2004**, *108*, 8161−8165.
(30) Hiller, J.; Rubner, M. F. *Macromolecules* **2003**, *36*, 4078−4083.
(31) Yang, S. Y.; Rubner, M. F. *J. Am. Chem. Soc.* **2002**, *124*, 2100−2101.

Chart 1. Equivalent Circuit Used for This Investigation

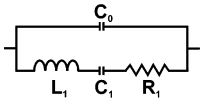

ethanolic MEA solution (95% ethanol) for 24 h. Following MEA functionalization, the substrates were rinsed and stored in ethanol and were used within 7 days. Prior to alternate layer deposition, the substrates were rinsed with DI H_2O and dried under a stream of N_2 gas.

Impedance analysis was performed as previously described.[33−36] The network parameters of an MEA-functionalized quartz crystal were analyzed using a Hewlett-Packard E5100A network analyzer in impedance-reflection mode. The network parameters of the crystals were measured by scanning 800 points over the frequency range of 5.0 MHz ± 100 kHz. The admittance (Y) and the phase angle (θ) of the quartz crystal were monitored and used to calculate the series resistance (R_1), capacitance (C_1), inductance (L_1), and frequency (f_s), as well as the parallel frequency (f_p) and capacitance (C_o), as previously described.[33] Chart 1 shows the four-component equivalent circuit representation of the piezoelectric element used in these studies. These data points were collected over time by acquiring values at a rate of 1 measurement/s using a program written in-house in the LabVIEW 5.0 environment. Following characterization of the MEA-functionalized quartz crystal, the substrate was removed from the measurement fixture and securely attached to a glass coverslip, via double-sided tape contacting the nonmetalized regions of the crystal. This assembly was then placed on the vacuum chuck of a spin coater (Specialty Coating Systems, model P6700), and spun at 3000 rpm. Ten drops of an aqueous, pH 6.5, 10% (v/v) microgel solution was added to the metalized region of the crystal. The substrate was allowed to spin for 15 s following microgel addition. The spinning substrate was then rinsed copiously with DI water and allowed to spin for an additional 15 s. Following rinsing, a layer of PAH was deposited by adding 10 drops of an aqueous, pH 6.5, 0.0526 monoM (mol/L monomer) solution followed by an additional 15 s of spinning. The substrate was then rinsed with DI water, and subsequent polyelectrolyte layers were added, as described above. An idealized schematic depiction of the thin-film configuration is shown in Figure 1. The quartz crystal can be removed from the tape holding it to the glass substrate at any time to allow for measurement of the network parameters. In all cases, the film was dried under a light stream of N_2 gas prior to measurement. The procedure of removing the crystal from its measurement fixture has been shown not to affect the network parameters of the crystal (data not shown). After the network parameters of the dry film were measured, a 10 μL drop of the desired pH solution, either pH ~3.0 or pH ~6.5 (1.0 mM ionic strength), was added to the film, and the network parameters were remeasured. Evaporation of the pH solution from the metalized region of the quartz crystal is negligible over the time scale of the experiment. The resulting network parameters can then be related to film mechanical properties, as previously described.[36−39]

Surface Plasmon Resonance Spectroscopy. Surface plasmon resonance spectra were obtained using an instrument built in-house. This scanning angle instrument is equipped with a fiber optic coupled white light source and a fiber optic coupled photodiode array detector (Ocean Optics) for illumination and detection, respectively. Sample excitation and detection angles were controlled using a Newport Corp. motion controller (MM 3000) and rotation stages (495 CC) with 0.01° resolution. A photograph of the instrument is included in the Supporting Information. To perform SPR experiments, a 50 nm thick layer of Au was evaporated onto (3-mercaptopropyl)-trimethoxysilane (MPTMS)-functionalized glass coverslips using a Denton Vacuum DV-502A thermal metal evaporator. MPTMS was attached to the substrates by exposing Ar plasma cleaned glass (Harrick Scientific) to a 1% (v/v) ethanolic (200 proof ethanol) MPTMS solution for 2 h. This layer functions as a molecular adhesion layer, thus improving the adhesion of Au to the glass substrate. The Au-coated substrate was then exposed to a 1 mM, ethanolic MEA solution for 24 h to render the Au surface positively charged. These substrates were then used for scLbL deposition. To obtain SPR spectra, the uncoated side of the glass substrate was optically coupled to the bottom of a hemispherical prism using a drop of immersion oil and mounted onto a custom-made, temperature-controlled flow cell. White light was then introduced to the sample over a variety of angles, and the reflectance from the sample was monitored as a function of wavelength at a single angle. Sample SPR spectra are included in the Supporting Information.

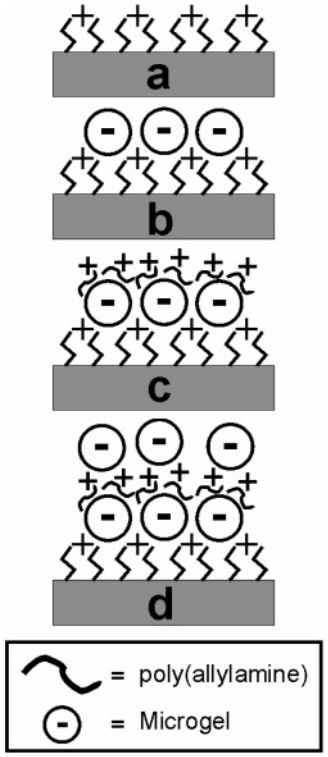

Figure 1. Schematic representation of the microgel thin films used in this investigation (not meant to imply order or morphology of the thin film): (a) blank, MEA-functionalized, Au substrate surface, (b) one layer of microgel added to the substrate, (c) addition of one PAH layer to the microgel surface, (d) subsequent addition of a microgel layer to the PAH surface. The PAH and microgel are not drawn to scale.

Microgel Synthesis. The same batch of microgels was used throughout this investigation. The microgels were composed of 88.5% NIPAm, 1.5% BIS, and 10% AAc and were synthesized via surfactant-free, aqueous free-radical precipitation polymerization as previously described,[16,40] using 140 mM total monomer concentration. Polymerization was carried out in a three-neck, 100 mL round-bottom flask to which was added 100 mL of a filtered, aqueous solution of NIPAm and BIS. This

(32) Palegrosdemange, C.; Simon, E. S.; Prime, K. L.; Whitesides, G. M. *J. Am. Chem. Soc.* **1991**, *113*, 12−20.
(33) Buttry, D. A.; Ward, M. D. *Chem. Rev.* **1992**, *92*, 1355−1379.
(34) Martin, S. J.; Granstaff, V. E.; Frye, G. C. *Anal. Chem.* **1991**, *63*, 2272−2281.
(35) Beck, R.; Pittermann, U.; Weil, K. G. *Ber. Bunsen-Ges. Phys. Chem.* **1988**, *92*, 1363−1368.
(36) Kanazawa, K. K. *Faraday Discuss.* **1997**, 77−90.
(37) Kim, J. M.; Chang, S. M.; Kwon, Y. S.; Muramatsu, H. *Synth. Met.* **1997**, *86*, 2263−2264.
(38) Kim, J. M.; Chang, S. M.; Muramatsu, H. *Polymer* **1999**, *40*, 3291−3299.
(39) Marxer, C. M.; Coen, M. C.; Greber, T.; Greber, U. F.; Schlapbach, L. *Anal. Bioanal. Chem.* **2003**, *377*, 578−586.
(40) Jones, C. D.; Lyon, L. A. *Langmuir* **2003**, *19*, 4544−4547.

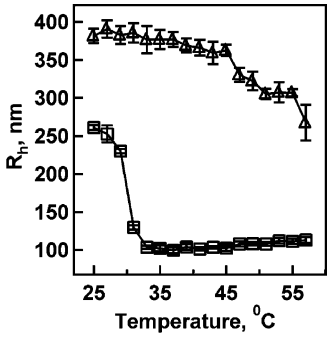

Figure 2. Volume phase transition curves taken from PCS measurements for the pNIPAm−AAc microgels used in this investigation, at pH 3.0 (squares) and pH 6.5 (triangles). Error bars represent 1 standard deviation about the average of five measurements.

solution was heated to ~70 °C while being purged with N_2 gas and stirred vigorously for ~1 h. After 1 h, AAc was added to the round-bottom flask to bring the total monomer concentration up to 140 mM. Once the AAc was added, the reaction was immediately initiated by injection of 1 mL of a hot (~70 °C), 2 mM aqueous APS solution. The solution immediately turned turbid, indicating successful initiation. This solution was heated and stirred for an additional 4 h under a blanket of N_2 gas. Following synthesis, the particles were purified by centrifuging the particle solution, decanting the supernatant solution, and resuspending in fresh H_2O. This process was repeated seven times.

Photon Correlation Spectroscopy. The temperature and pH responsivity of the pNIPAm-*co*-AAc microgels was confirmed by photon correlation spectroscopy (PCS; Protein Solutions Inc.) prior to their use for thin-film fabrication. PCS has previously been used as a tool for determining mean particle size and particle size distributions,[41] and has been used for these microgel systems in the past.[16,40] Briefly, a diluted microgel solution was added to a plastic cuvette and inserted into the PCS cuvette holder, which was equipped with a Peltier device for sample temperature control. Laser light (783.9 nm) was introduced to the sample via a single-mode optical fiber, and scattered light was collected by a fiber coupled avalanche photodiode detector at 90°. The random intensity fluctuations of the scattered radiation were used to calculate an autocorrelation decay, which can then be related to the particle translational diffusion coefficient (Dynamics Software version 5.25.44). The average hydrodynamic radius was then calculated using the Stokes−Einstein equation. For these measurements, each sample was allowed to equilibrate at each temperature for 20 min. At each temperature, 5 consecutive runs were performed, where each run was composed of 15 individual radius measurements using a 30 s integration time for each measurement.

Results

Figure 2 shows temperature-dependent PCS data for the microgels used in this investigation at acidic (~3.0) and approximately neutral (~6.5) pH values. From the figure it can be seen that, under acidic conditions (pH < pK_a), the microgels have an average R_h of ~260 nm. Since the AAc groups are almost fully protonated at this pH, the microgels undergo a continuous VPT over a ~6 °C range, with a lower critical solution temperature (LCST) of ~31 °C. From Figure 2 it is observed that, at pH ≈ 6.5 (pH > pK_a), the microgels have an average R_h of ~375 nm. The swelling of the microgels at this pH is expected due to deprotonation of the majority of the AAc groups, which introduces charge−charge repulsion and increased osmotic pressure in the network. Furthermore, as the microgels are heated in pH 6.5 solution, they are unable to deswell to the same minimum R_h observed at pH 3.0, and the VPT temperature is much higher, again due to the charged nature of the microgel network.

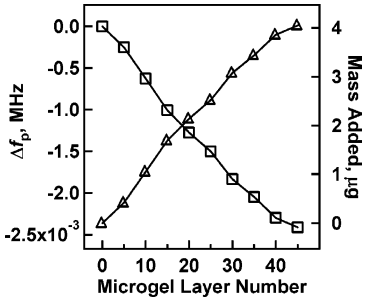

Figure 3. Δf_p (squares) and added mass (triangles) values as a function of the microgel layer number obtained from QCI measurements.

Since the microgels are negatively charged at pH 6.5, scLbL was performed at this pH. This ensures the strongest polyelectrolyte interactions during layer buildup, and should result in a denser film. Layer buildup was monitored via QCI. These measurements were performed by measuring the initial network parameters of the MEA-functionalized quartz crystal in air. Following this measurement, the crystal was removed from its measurement fixture, and five layers of microgel and four layers of PAH were spun onto the crystal in an alternating fashion, as described in the Experimental Section. The crystal was then dried under a stream of N_2 gas and placed back in the measurement fixture to allow the new network parameters to be measured. This process was repeated for every five microgel layers. Shown in Figure 3 is a plot of the change in resonant frequency of the crystal oscillating in air (Δf_p) as a function of microgel layer number; the resonant frequency decreases linearly with increasing film thickness. Figure 3 also shows the corresponding changes in mass as calculated from Δf_p values using eq 1. The Sauerbrey equation relates mass changes directly to Δf_p assuming the microgel thin film is behaving as a rigidly attached overlayer. Using this simple formalism, the total frequency change following the addition of 45 microgel layers corresponds to ~4.0 μg of added mass, or 0.44 μg per 5 microgel/4 PAH layers. We estimate that ~0.299 μg should be added to the crystal surface for each microgel layer, assuming deposition of a close-packed monolayer of microgels, where each microgel is assumed to have a polymer content of 5% by mass. This corresponds to 1.495 μg of added mass for every five microgel layers, without considering the mass of the PAH added for each layer. The discrepancy between the experimental results and the predicted values is most likely due to the lack of truly close packed microgel layers.

Another way to represent these data is by showing the full impedance spectra obtained during the frequency sweep. Figure 4 shows plots of the phase angle (θ) and the logarithm of the admittance (log Y) as a function of frequency for a crystal functionalized with MEA only, as well as 10- and 40-layer films. These curves were obtained in air. Plots of Y vs frequency are

(41) Pecora, R. *Dynamic Light Scattering*; Plenum Press: New York, 1985.

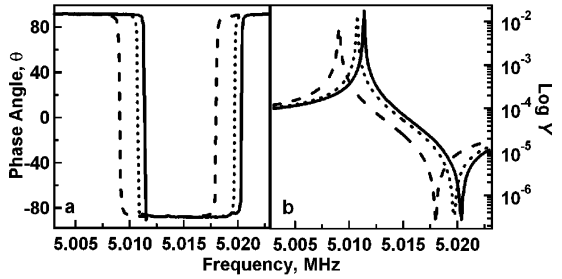

Figure 4. Quartz crystal θ (a) and log Y (b) behavior for an MEA-functionalized crystal (solid line) and 10-layer (dotted line) and 40-layer (dashed line) microgel films.

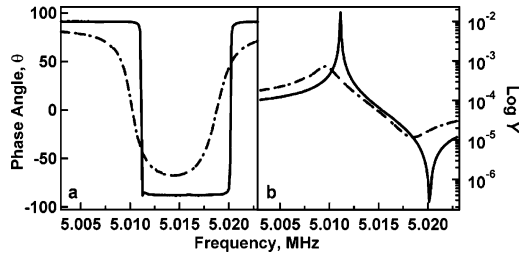

Figure 5. Quartz crystal θ (a) and log Y (b) behavior as 10 μL of pH 3.0 (dotted line) and 6.5 (dashed line) solution is added to a blank, MEA-functionalized quartz crystal surface (solid line = air oscillation).

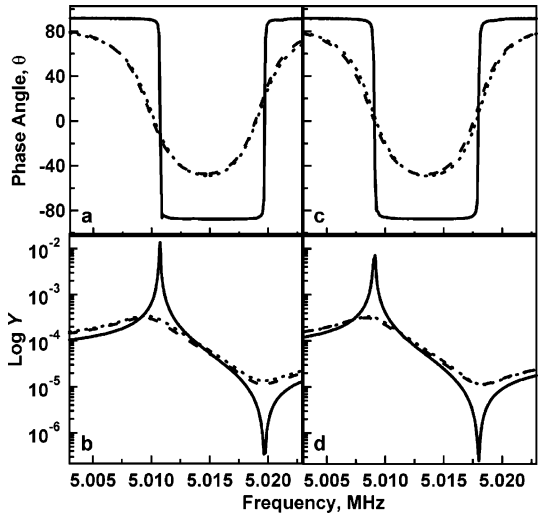

Figure 6. Quartz crystal θ (a, c) and log Y (b, d) behavior as 10 μL of pH 3.0 (dotted line) and 6.5 (dashed line) solution is added to a 10-layer (a, b) and 40-layer (c, d) microgel thin film (solid line = air oscillation).

included in the Supporting Information. The shifts to lower frequency with added mass that are observed for both sets of curves again indicate a decrease in resonant frequency. Also, the curve shapes do not change significantly with layer addition, suggesting little or no dampening of the crystal oscillation. However, if a blank, MEA-functionalized crystal is exposed to pH 3.0 and 6.5 solutions, the crystal's θ and log Y behaviors are observed to become dramatically different. Figure 5 shows these data, where it can be seen that the crystal oscillation becomes extremely dampened as indicated by the very broad θ and log Y curves. Note that this behavior is pH independent. Figure 6 shows the phase angle and admittance spectra for the 10- and 40-layer microgel thin films. In panel a we see that the θ curve for the 10-layer film in air is very similar in shape to

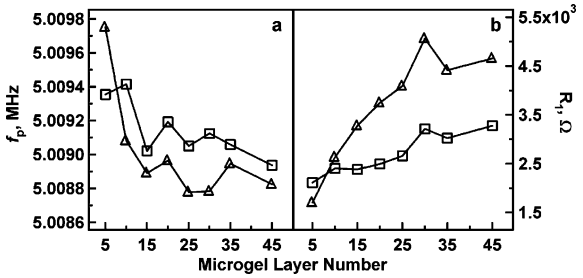

Figure 7. Quartz crystal network parameters f_p (a) and R_1 (b) as a function of the microgel layer number at pH 3.0 (squares) and 6.5 (triangles).

the spectrum obtained from the blank crystal in air (Figures 4 and 5). As in the case of the MEA-functionalized crystal, when the microgel films are exposed to pH 3.0 and 6.5 solutions, the curves become very broad due to dampening of the oscillation. The dampening of the crystal oscillation is also evident in the admittance spectra shown in panels b and d. From the plots of θ and log Y it is difficult to resolve a difference in curve position or shape as a function of pH, but the shift in the position of the curves relative to that for the respective film in air is quite obvious. From Figure 6a,c it is observed that the 10-layer film is more sensitive to solution addition relative to the 40-layer film, as evidenced by a larger negative frequency shift in θ. Indeed, the frequency at which the phase angle crosses zero is almost unchanged during solution addition in the case of the 40-layer film.

The dependence of f_p and the resonant resistance (R_1) on the layer number and pH are shown in Figure 7. The figure shows that the magnitude of f_p decreases as a function of the layer number and plateaus at ~20 microgel layers while R_1 increases over the whole range. This behavior is indicative of a film that is becoming more viscous, i.e., less swollen, with layer number.[34,42–44] Furthermore, the values of f_p and R_1 are lower and higher, respectively, at pH 6.5 relative to pH 3.0. Table 1 lists the differences in network parameter values for films exposed to pH 3.0 and 6.5 solutions, compared to their respective network parameters in air. These data show that the f_p and R_1 values are shifted more when the films are exposed to pH 6.5, as compared to pH 3.0. Table 1 also includes values of Q calculated using eq 2.[38]

$$Q = 1/R_1(L_1/C_1)^{1/2} \quad (2)$$

Q is a general figure of merit for the quality factor of an oscillator, with larger values indicating less dampened (narrower frequency response) oscillation. The numbers used in this calculation come from the equivalent circuit model presented in Chart 1 and the corresponding network values, which are given in the Supporting Information. Using this formalism, we find that Q is significantly lower at pH 6.5 for the 20- and 30-layer films, again suggesting a more viscous, or dampening, layer.

(42) Kanazawa, K. K.; Gordon, J. G. *Anal. Chem.* **1985**, *57*, 1770–1771.
(43) Kanazawa, K. K.; Melroy, O. R. *IBM J. Res. Dev.* **1993**, *37*, 157–171.
(44) Lee, S. W.; Hinsberg, W. D. *Anal. Chem.* **2002**, *74*, 125–131.

Table 1. Network Parameters for Microgel Films Exposed to pH Solutions

microgel layer no.	Δf_p,[a] MHz (pH 3.0/6.5)	ΔR_1,[a] Ω (pH 3.0/6.5)	Q[b] (pH 3.0/6.5)
10	−0.00122/−0.00155	2324/2555	1726/1778
20	−0.00081/−0.00104	2294/3550	1630/1178
30	−0.00038/−0.00073	2995/4845	1148/864

[a] Values calculated by subtracting f_p for the respective microgel films in air from f_p obtained by exposing each film to pH 3.0 or 6.5 solution. [b] Calculated using eq 2 from the absolute values for R_1, C_1, and L_1 (Supporting Information).

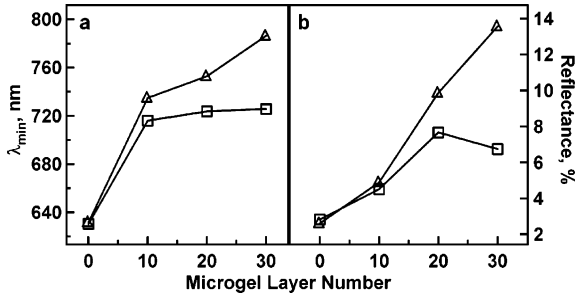

Figure 8. λ_{min} (a) and percent reflectance (b) as a function of the microgel layer number in response to pH 3.0 (squares) and 6.5 (triangles) solutions.

Surface plasmon resonance analysis performed on similar films displays a similar trend. Figure 8 shows plots of the SPR reflectance wavelength minimum (λ_{min}) and percent reflectance values as a function of the microgel layer number at pH 3.0 and 6.5. For these experiments all films were assembled on MEA-functionalized, Au-coated, glass substrates similar to the substrates used for QCI experiments. Following assembly of a given number of microgel layers, the substrate was attached to a hemispherical prism and coupled to the temperature-controlled, fluid flow cell of the SPR instrument. The experiments were conducted at room temperature while the reflectance spectrum from the substrate in contact with either pH 3.0 or pH 6.5 solution was monitored. During the experiment, the light excitation and detection arms were held constant at 73° relative to the prism normal. Full reflectance spectra as a function of the layer number and pH can be seen in the Supporting Information. Figure 8a shows that, when a 10-layer microgel film is exposed to pH 3.0, λ_{min} increases by ∼90 nm compared to that of a blank substrate exposed to a pH 3.0 solution. If pH 6.5 solution is introduced to the same 10-layer film via the fluid flow cell, λ_{min} further increases by ∼20 nm. Figure 8b shows that the percent reflectance from the 10-layer film increases from ∼2.8% to ∼4.5% upon pH 3.0 and 6.5 exposure, respectively. As the number of microgel layers is increased from 10 to 20, the λ_{min} of the film at pH 3.0 increases by ∼5 nm, while the λ_{min} of the same film exposed to pH 6.5 solution changes by ∼20 nm. If the percent reflectances of the film at pH 3.0 and 6.5 are compared, it can be seen that the film at pH 6.5 displays a higher percent reflectance than the film at pH 3.0, indicating that the film at pH 6.5 scatters more light, or is more lossy than the film at pH 3.0. Similar SPR behavior is also observed for a 30-layer microgel thin film.

The results of repeated pH cycling on the film optical properties are shown in Figure 9. For a 10-layer film, the shift in λ_{min} was ∼20 nm upon changing the solution

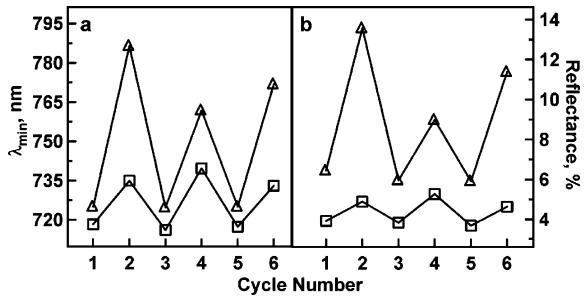

Figure 9. λ_{min} (a) and percent reflectance (b) values as 10-layer (squares) and 30-layer (triangles) microgel films are alternatively exposed to pH 3.0 (odd numbers) and 6.5 (even numbers) solutions.

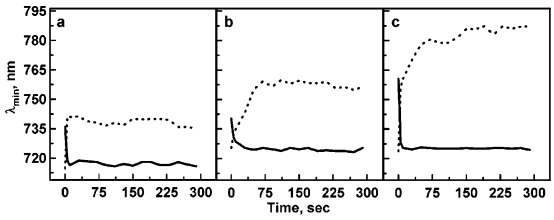

Figure 10. λ_{min} over time for 10-layer (a), 20-layer (b), and 30-layer (c) microgel thin films upon introduction of pH 3.0 (solid line) and 6.5 (dotted line) solutions.

pH from 3.0 to 6.5 while the percent reflectance increased by ∼1%. Conversely, the 30-layer film λ_{min} shifts by ∼60 nm while the percent reflectance changes by ∼7% as the solution pH is changed from 3.0 to 6.5. The shifts observed for the 30-layer film are not as reproducible as in the 10-layer case.

To investigate the kinetics of film equilibration during pH changes, λ_{min} was measured as a function of time following the pH switch. These data are presented in Figure 10. Panel a illustrates that, when a 10-layer film is exposed to a pH 6.5 solution, λ_{min} reaches its equilibrium value of ∼740 nm in ∼5 s. When the solution pH is changed to 3.0, λ_{min} decreases to its equilibrium value of ∼715 nm again in ∼5 s. However, for a 20-layer film to reach its equilibrium value of ∼760 nm at pH 6.5, ∼75 s of equilibration time is required. The equilibrium value of ∼720 nm is reached in less than 40 s upon pH 3.0 solution addition. Figure 10c shows that, when a 30-layer film is exposed to pH 6.5, λ_{min} increases quickly within the first 20 s, followed by a slow component, ultimately reaching its equilibrium value of ∼785 nm in ∼300 s. When this film is exposed to pH 3.0, the λ_{min} decreases and reaches its equilibrium value of ∼725 nm in less than 10 s. Qualitatively, these data indicate that the film kinetics are roughly independent of the layer number (fast kinetics) on going from pH 6.5 to pH 3.0. However, the kinetics appear to become more sluggish with increasing layer number for switches from pH 3.0 to pH 6.5.

Discussion

QCI crystals, with their Au electrodes functionalized with MEA, were used to monitor scLbL deposition as microgel layers were added to the crystal. As can be seen from Figure 3 the mass added to the QCI crystal increased linearly as microgel layers were added to the substrate surface. These data are indicative of a reproducible buildup mechanism that is expected for layers

assembled using LbL assembly techniques. If scLbL deposition did not result in a consistent particle density per layer for these thin films, the linear behavior seen in Figure 3 would not be observed. The θ and log Y behavior of a QCI crystal as a function of the microgel layer number shown in Figure 4a,b illustrates that the blank QCI crystal exhibits the expected sharp resonance behavior indicative of a crystal that is experiencing very low losses, with typical Q values of ~35000. It can also be seen from Figure 4a that as microgel layers are added to the QCI crystal the phase behavior remains fairly sharp; i.e., low losses are experienced, but are shifted to lower frequency, indicative of mass loading. The log Y plots, Figure 4b, for a microgel thin film loaded QCI crystal showed curves that are also shifted to low frequency and have a slight decrease in amplitude of Y, while still maintaining high Q values (~25000).

As expected, crystal oscillation in solution results in dampened oscillation, as seen in Figure 5. This behavior is a well-known effect of oscillation dampening/energy loss of a QCI crystal in contact with a solution and has been explained by researchers such as Kanazawa, Buttry, and Ward to be due to viscous loading of the liquid on the crystal.[33,42,45,46] Viscous loading has been shown to affect the QCI crystal resonant oscillation frequency in a solution-viscosity-dependent fashion; i.e., more viscous solutions are able to shift the resonant frequency to lower values than a less viscous solution.[42,45] From the figure it is also important to note that the curves for the crystal in contact with pH 3.0 and pH 6.5 solutions are overlapped, indicating that the response of the blank quartz crystal is not pH sensitive.

These viscous loading effects become more prevalent when the crystal is coated with microgel multilayers. Figure 6 shows the θ and Y response of a crystal composed of 10 and 40 microgel layers as a function of pH solution addition. From Figure 6a,b it can be seen that the θ and Y behavior of a dry, 10-layer film in air is similar to that of a blank, MEA-functionalized crystal in air with a characteristically high Q factor (~35000) but shifted to lower frequency. However, immersion of the films in aqueous media results in significant damping, as evidenced by the broadening of both the θ and Y responses. If the network parameters f_p and R_1 are plotted as a function of the layer number upon exposure of the films to pH 3.0 and 6.5 solutions (Figure 7), the difference in crystal behavior becomes apparent. As can be seen from the figure, and as outlined in Table 1, the values of f_p and R_1 are shifted more for a film at pH 6.5 for almost every layer number. For example, f_p is shifted to a lower frequency for a film exposed to a solution of pH 6.5 versus pH 3.0, while the crystal oscillation is more resistive at pH 6.5 versus pH 3.0. This behavior can be understood by taking into account the differential ionization of weak polyelectrolytes AAc and PAH as a function of pH.[24,27,30,31] At pH 3.0 the AAc groups on the microgel will be almost fully protonated as will be the PAH. This should decrease the interaction between the now neutral particle and cationic PAH, which results in film swelling. If on the other hand a pH 6.5 solution is added to the film, the AAc groups become almost fully charged while the PAH stays mostly ionized ($pK_a \approx 9.0$), thereby enforcing the PAH−AAc complexation. A more highly complexed film results in a more viscous film as indicated by the measured resonant frequency and resistance values. This hypothesis can be verified from the calculated Q values as a function of the layer number and pH as seen in Table 1. From this it can be seen that the Q value decreases with layer number and, with the exception of the 10-layer film, is lower at pH 6.5 than at pH 3.0. This trend in the value of Q is indicative of a film that is more viscous with layer number and increasing pH.[34] A viscosity increase with layer number suggests that the film becomes denser as more layers are added.

This behavior was confirmed by probing the local optical properties of the film in response to pH using SPR, which is a well-known and studied technique for probing optical densities and has previously been exploited for similar films.[12,13,47,48] The data shown in Figure 8a reveal the fact that a film exposed to pH 3.0 is less optically dense, i.e., more water swollen, than the film at pH 6.5 as noted by a smaller shift in λ_{min} for a film exposed to pH 3.0 solution. The differential solvation behavior is also evident in the larger percent reflectance values for a film exposed to a pH 6.5 solution, as opposed to a pH 3.0 solution, indicating that the film is more lossy due to scattering from refractive index heterogeneities. Figure 9 shows the reproducibility of the pH-dependent film solvation for 10- and 30-layer films. This behavior is noted by the oscillatory behavior in λ_{min} and percent reflectance indicative of a film that is able to dynamically change solvation in a pH-dependent fashion. This behavior is shown to be reproducible over at least six pH cycles. The kinetics of film solvation state switching were also monitored via SPR, where it is expected that films of lower layer number should respond to pH switching faster than films composed of more layers. Shown in Figure 10 are the data illustrating this point. From Figure 10 it can be seen that the films at pH 3.0 all swell very fast compared to film deswelling upon exposure to pH 6.5 solution. By comparing the panels in Figure 10, the film-thickness-dependent swelling kinetics can be observed, where the 10-layer film changes solvation the fastest, followed by the 20- and 30-layer films upon pH 6.5 solution introduction. This behavior is expected, at least qualitatively, given the fact that film deswelling is dependent on ion transport, water diffusion, and film reorganization, all of which should increase in time with film thickness. Conversely, film swelling is less dependent on film reorganization, as disruption of the PAH−AAc interactions should be faster than re-formation of the complexes following a pH jump.

Conclusions

From this investigation, QCM and SPR studies reveal that polyelectrolytic microgel thin films are pH-sensitive materials that switch their solvation state depending on whether the film is exposed to a pH solution where the attractive forces were enforced (pH 6.5) or disrupted

(45) Kanazawa, K. K.; Gordon, J. G. *Anal. Chim. Acta* **1985**, *175*, 99−105.
(46) Ward, M. D.; Buttry, D. A. *Science* **1990**, *249*, 1000−1007.
(47) Harmon, M. E.; Kuckling, D.; Frank, C. W. *Macromolecules* **2003**, *36*, 162−172.
(48) Kuckling, D.; Harmon, M. E.; Frank, C. W. *Macromolecules* **2002**, *35*, 6377−6383.

(pH 3.0). This behavior scales with the layer number, where a film containing more microgel layers is less sensitive to solution addition than a film with fewer layers. It is also shown that a film with a given layer number at pH 6.5 is able to affect the network parameters of a QCI crystal more than a film exposed to pH 3.0 solution, which is indicative of a pH-dependent film viscosity. The films are also able to switch their solvation state over at least six pH cycles, where the kinetics of swelling/deswelling are dependent on the microgel layer number. It is interesting to note that, while AAc protonation causes film swelling, it does not apparently lead to complete film dissolution via disruption of all the PAH−AAc interactions. We tentatively ascribe this to polymer entanglements within the film, which the above data indicate are comprised of highly interpenetrated PAH/ microgel interactions. Future studies are aimed at investigating the detailed molecular-level structure of these complex microstructured films.

Acknowledgment. L.A.L. acknowledges support through an NSF-CAREER award (Grant CHE-9984012) for this work. Support is also acknowledged from the Alfred P. Sloan Foundation Fellowship and from a Camille Dreyfus Teacher-Scholar Award. Cryo-SEM analysis of microgel thin films was performed by Dr. Robert Apkarian at the Emory University Integrated Microscopy and Microanalytical Facility.

Supporting Information Available: Full SPR spectra, a photograph of the SPR instrument, linear Y plots for films in air and exposed to pH 3.0 and 6.5 solutions, R_1 vs f_p plots as a function of the layer number, and absolute values for the network parameters for films exposed to pH 3.0 and 6.5 solutions (PDF). This material is available free of charge via the Internet at http://pubs.acs.org.

CM048844V